DEXARM ENGINEERING MODEL DEVELOPMENT AND TESTING

A. Rusconi [(1)]; P. Magnani [(1)]; P. Campo [(2)]; R. Chomicz [(3)]; G. Magnani [(4)] ; C. Lambert [(5)] ; G. Gruener [(6)]

[(1)] Selex Galileo
Via Montefeltro, 8 - 20156 Milano (ITALY)
email: andrea.rusconi@selexgalileo.com
email: piergiovanni.magnani@selexgalileo.com

[(2)] SENER Ingeniería y Sistemas S.A.,
Avda. Zugazarte, 56 - 48930 Las Arenas (SPAIN)
email: pablo.campo@sener.es

[(3)] Tecnomare S.p.A.,
S. Marco, 3584 - 30124 Venezia (ITALY)
email: roman.chomicz@tecnomare.it

[(4)] Politecnico di Milano
Dipartimento di Elettronica e Informazione
Piazza L. da Vinci, 32, Milano (ITALY)
email: magnani@elet.polimi.it

[(5)] Oerlikon Space AG,
Schaffhauserstrasse 580, 8052 Zürich (SWITZERLAND)
email: christian.lambert@oerlikon.com

[(6)] CSEM
Untere Gründlistrasse 1, 6055 Alpnach Dorf (SWITZERLAND)
email: gabriel.gruener@csem.ch

INTRODUCTION

The goal of the DEXARM project [1] is the development of a robot arm comparable in size, force and dexterity to a human arm, to be used for space robotics applications in which the manipulation/intervention tasks were originally conceived for humans. These applications are typically external or internal servicing of orbiting platforms or robotics for planetary exploration. The first user programme currently envisaged for DEXARM is EUROBOT [2].

The main challenges of this development lay in the minimisation of resources that the applications require. To achieve this goal, ESA has encouraged the exploitation of innovative approaches and technologies to drastically minimise mass, volume and power consumption while providing adequate performance (output torque capability and positioning accuracy/repeatability).

The DEXARM project has been divided into three phases:

- Phase 1: DEXARM definition
  This phase comprises system requirement definition, system architectural design and specification of requirements for sub-systems, preliminary design of joint (evaluating different architectures);
- Phase 2: Joint development
  This phase consists of detailed design, development, manufacturing and test of one joint prototype;
- Phase 3: DEXARM development
  Upon possible design iterations based on the joint prototype test results from phase 2, phase 3 is focused on the development and manufacturing of joints, limbs and structures, assembly and integration in a dextrous robot arm system testbed, validation by system-level testing and demonstration.

Phases 1 and 2 have been completed. This paper describes the main results achieved during phase 3 of the project (which is under completion).

ARM CONFIGURATION

In phase 1, an extensive kinematics and geometrical analysis has been conducted, after which the most promising kinematics structures have been identified.
In order to select a reference architecture, the following analyses have been carried out: workspace and dexterity, trajectory execution on typical paths, kinematics and static performance at the end effector. Furthermore, other design aspects have been evaluated, such as arm folding and volume constraints, modularity, cable routing, mass, complexity of manufacturing and wrist envelope.
Five configurations were preliminarily selected and deeply analysed [1]. Two of them were selected as best candidates.
In phase 3, the final choice has been made, also re-considering additional wrist solutions, based on the offset wrist (where joint 7 is mounted in offset and retracted position, to minimise wrist length).
The overall selection process is shown in Fig. 1.

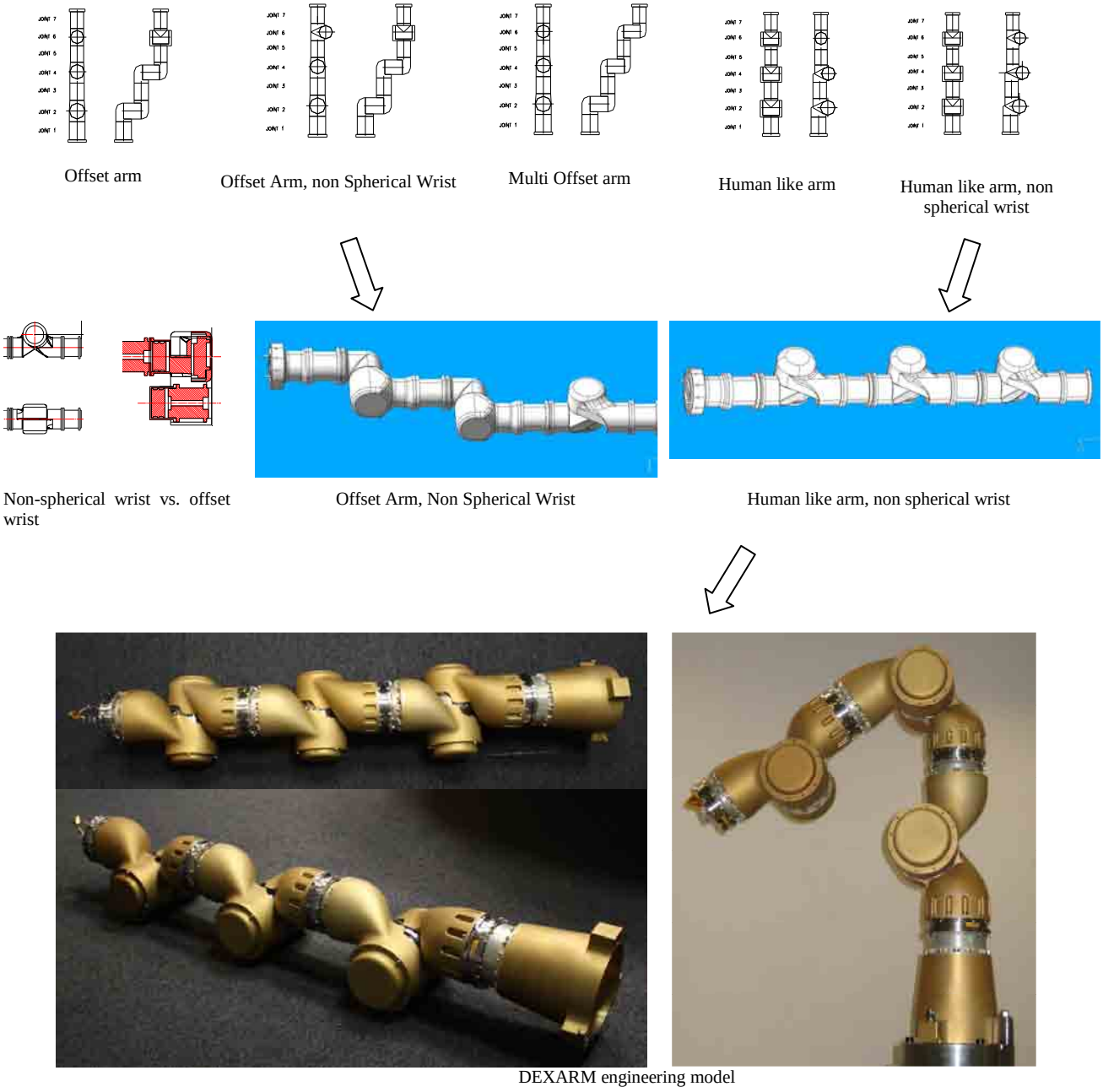

Fig. 1. Arm configuration selection process

The final trade-off led to the following considerations:

- In terms of dexterity and mass, there is no significant difference between the two architectures;
- Volumetric considerations (encumbrance) and design modularity indicated that there is an advantage in the human like arm with non spherical wrist.

The offset (retracted) wrist instead gives a significant advantage in dexterity, while it might create a problem in terms of clearance and a need for posture reconfiguration during trajectory execution. For this reason, it was discarded.
Based on the above considerations, the human like arm with non spherical wrist has been selected as DEXARM reference architecture.

ARM CHARACTERISTICS

The main DEXARM characteristics are summarised here below:

- Functional and performance characteristics:
  - lightweight dextrous robot arm;
  - redundant kinematics (7 joints, with angular range of ±175º for roll joints, -175º..+45º for pitch joints);
  - force-torque capability of 200 N and 20 Nm at the arm tip;
  - payload handling capability of 10 kg at 1-g;
- Physical characteristics:
  - mass of about 25 kg;
  - power consumption of about 100 W;
  - length of 1.2 m;
- Operational characteristics:
  - capability of performing 1-g operations without using any special off-loading device;
  - EVA operability (attach-detach DEXARM from user platform, back-drive the joints without the use of any special tool);
- Safety:
  - space station safety requirements are applicable, requiring special attention to robotic related hazards like possibility of collision with other space station elements.

BASE

The arm base provides mechanical and electrical connection with the user platform (e.g. EUROBOT). The arm is required to be attached/detached by the astronaut in EVA, therefore the design includes three captive fixation bolts (with EVA standard 7/16in heads) and mechanical alignment provisions for installation on the user platform, allowing mechanical and electrical connection.
Estimated mounting time is in the order of ten minutes. The fixation bolts are within visibility of the astronaut, so that the mating status can be visually verified. If required by the on-orbit vibration environment, means to avoid inadvertent back out of the bolts can be implemented (e.g. by provision to lock bolt heads after fixation).
Connector mating force is estimated to be about 50 N, a value that is compatible with EVA capabilities.
The arm base is shown in Fig. 2.

Fig. 2 Arm base

LIMBS

The limbs are the connecting elements between the DEXARM joints. As such they have to be stiff, allow repeated mounting and dismounting operations, protect harness and internal electronics against outer environment, carry loads from one hinge to the next (main load transfer path). In addition, their geometry must be compatible with a wide joint angular range and allow a dimensional transition from a large shoulder joint to a reduced wrist joint.
The design of the limbs has been aimed at minimising mass and volume of the arm, while keeping adequate stiffness and load capability. To also comply with the requirement on arm length, a tight integration with joints and electronics components has been pursued. The achieved result can be appreciated in Fig. 3.

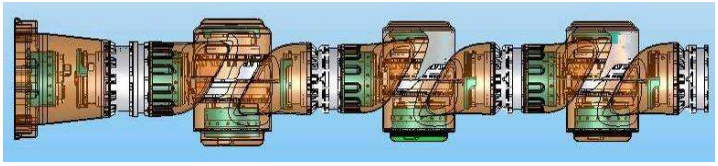

Fig. 3 DEXARM internal component view – tight integration between limbs, joints and electronics

The full set of limbs has been developed in Aluminium. Mill machining processes have been utilised for the construction and the achieved mass value has been further reduced through a final optimisation on the physical limbs themselves. The baseline aluminium limbs are shown in Fig. 4.

Fig. 4 Aluminium limbs 1 and 2

Design of the arm with Carbon Fiber Reinforced Plastic (CFRP) limbs has also been performed and two specific limbs (limb 3 and 5) have been developed also in CFRP to allow comparison between different technologies. Specifically, limb 5 is shown in Fig. 5.

The interfaces of the limbs to the joints have been implemented by means of L-shaped Aluminium fittings, bonded to the CFRP parts and bolted to the joint interfaces. The electrical bonding has been implemented by means of a wire with convex contact stud.

CFRP limbs have been subject to functional (load, stiffness, etc.), thermal cycling and vibration test. They successfully withstood the applied loads without any plastic deformation of metallic components or failure within composite components.

Fig. 5 CFRP limb 5

In terms of mass about 0.7 kg saving is estimated when employing CFRP limbs (passing from about 3.4 kg to 2.7 kg for six limbs). The gain in mass would become more evident in case of a longer arm (2-3 m).

CFRP limb 3 has been equipped with a release mechanism which can be used by the EVA to fold the arm in contingency situation, by mechanical means only (without relying on any control electronics).

The release mechanism has six segments with a u-shape cross-section. They are arranged around two interface-rings. Each ring has a conical collar. The diameter of this arrangement is reduced when the segments and their integrated spanning-bolts are tightened. The segments “slide” along the slanted collar and clamp the whole system. When the bolts are un-tightened the segments will separate with help of helical-springs between each segment and un-clamping of the system results. The bolts and threads are designed such that they are “unloosable”.

Fig. 6 Release mechanism

JOINTS

In phase 2, a joint prototype has been developed and tested. It is a highly sensorized integrated joint, composed of mechanics, electronics and joint control software.
At the beginning of phase 3, a joint re-engineering activity has been performed, to implement and validate specific design modifications identified during prototype integration and test.
In parallel with re-engineering, the joint design has been scaled for the joints of different sizes as needed in the arm. Two joint sizes have been developed: a shoulder joint, targeted to a 200 Nm torque, and an elbow/wrist joint, targeted to a 100 Nm torque. A smaller wrist joint (40 Nm) was considered also, but the gain in terms of mass and dimensions would have been slight, with respect to the decrease in torque capability. In addition, it has been considered beneficial to have a strong wrist (with 100 Nm joints), to better implement EUROBOT application requirements, where the arm can actually be used as a leg (e.g. to walk on ISS handrails and not only to manipulate objects).
The joint mechanical design is based on a minimum number of structural parts, where all components are tightly integrated together to minimise mass and volume requirements. All joints of a given size are completely identical in terms of physical and performance parameters, with exception of range of travel and end stop location. The joint type (roll or pitch) can be switched by changing its end stops.
Each joint is functionally and physically divided in two operative subassemblies, input and output, whose performance can be tested independently. The two subassemblies are fully interchangeable from one joint to another within the same mechanical size. The input subassembly or high speed subassembly includes all the parts before the reducer. This subassembly is not in the structural path and is characterised by high speed and low torque. The aim of the subassembly is to provide controlled motion to the Harmonic drive wave generator. The output subassembly or low speed subassembly includes the joint structural elements, providing support and powerful torque transmission to the next elements in the kinematics chain. The two joint sizes are shown in Fig. 7. The mass of each joint is about 2.2 kg for the elbow and 3.2 kg for the shoulder.

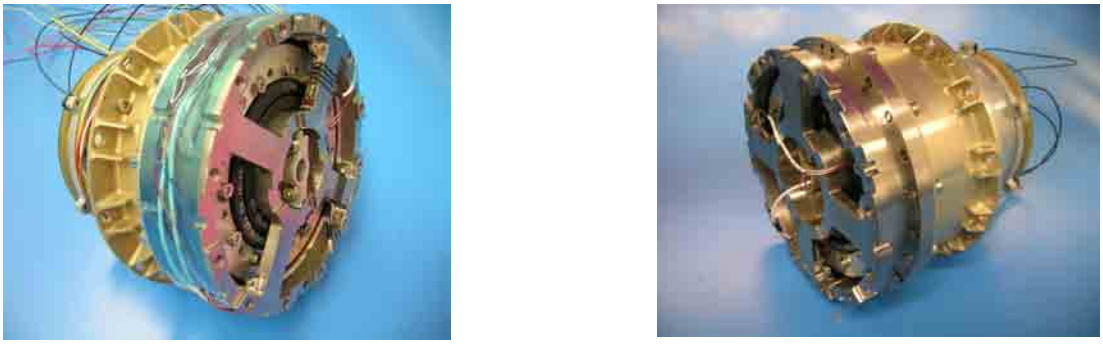

Fig. 7 Joints – elbow and shoulder size

Electro-mechanical components

A description of the main joint components is given here below:

- Motor: three phase DC brushless motor;
- Brake: electromagnetic fail-safe brake;
- Gear: Harmonic Drive;
- Bearing system: a preloaded pair of ball bearings has been employed for the output shaft, while super-duplex ball bearings have been employed for input shaft of the joint;
- Motor position sensor: electrical encoder, capable of providing accurate shaft position information so to implement sinusoidal commutation and velocity control;
- Output position sensor: a resolver has been employed, with a large central hole allowing a very high output shaft stiffness and not requiring excessive mounting accuracy in the relative position of its rotoric part with respect its statoric part;
- Torque sensor: torque sensing has been implemented by means of four strain gauges organised in full bridge, applied to the ribs of a duly machined output flange. The optimum design of the output flange with torque sensor is a trade-off between sensing accuracy and joint stiffness and load capability, since these two requirements are directly in opposition. The choice was to design a robust output flange, with a stiffness at least five times higher than the Harmonic Drive stiffness, and to obtain the required sensor accuracy through the use of a high performance instrumentation amplifier in the acquisition electronics.

Thermal design

The thermal design of the joint has been driven by placing the important power dissipative items (motor stator, power MOSFETs) tightly connected to the outer case to reduce thermal path resistance to the outer environment.

Electronics

Each joint electronics is a node on the DEXARM power (28 V) and data bus (CAN bus). This distributed architecture, with the electronics integrated with the joints, eliminates the need for multi-wire cable harnesses, thereby saving system mass and increasing system reliability, improves robustness with respect to EMC, having joint electronics located close to the sensors and the actuators, and still provides the needed data exchange frequency, satisfying control system bandwidth requirements. The joint electronics is composed of three circular boards, interconnected with flex cables, as shown in Fig. 8.

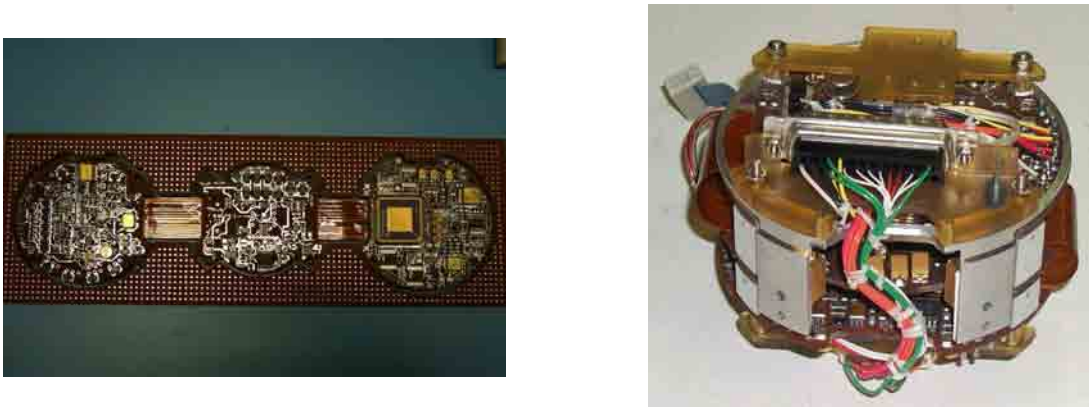

Fig. 8 Joint electronics boards, laid on a plain and folded during integration

The design of the electronics has been very challenging. Several design iterations were needed to reach the required dimensions and to optimise power consumption.
In phase 3, further improvements were performed. Modularity and easiness of integration have been enhanced, by employing interface connectors between joint mechanics and joint electronics (in phase 2, some cables, e.g. for motor and brake, were directly soldered on the electronics). Some electrical circuits have been updated, to increase robustness and further decrease power consumption. Hardware customisation for different joint sizes has been performed (brake, resolver, torque sensor and motor current sensing circuits). Finally, a local torque sensor PCB has been added, to be used as support for connecting strain gauge signals and for local amplification, to increase signal to noise ratio. Currently, the local amplification has been implemented for joint 7.

Joint servo control

Control software is embedded in the joint electronics [3]. It features several control schemes (current, velocity, torque, position and impedance) that can be configured based on the application needs. This gives maximum freedom for the implementation of the majority of control strategies present in the literature that can be used at Cartesian level.

In phase 3, some updates and improvements have been performed on the servo control software. The low level motor current control has been re-written with 32-bit fixed point, high accuracy mathematical functions. A dynamic handling of current loop saturation has been added, to make maximum usage of bus voltage and reach a joint speed (at no load) close to the theoretical value of 0.5 rad/s. Two options are now available for brake control: voltage control and current control. Best choice depends on the operating temperature.
Finally, new modes have been studied, related to power saving, namely a sleep mode and a high-energy/low-energy control mode.
If the arm is in standby for a substantial period of time, it might prove advantageous to have a sleep mode that puts each joint in a sleep state that saves as much energy as possible without switching it completely off. The benefit of a sleep mode being that waking up should be faster than the time required to switch on the joint. In this mode, command execution is suspended and all peripherals are turned off. However, an incoming CAN message will be detected and can be used to wake up the processor. Direct measurements on the joint show that the sleep mode allows to reduce power

consumption during standby from 4 W to 3.1 W, a reduction of 22%. More saving could be reached by introducing hardware modifications to switch off some unused power-auxiliary lines in sleep mode.
A high-performance (high-energy) controller would be the nominal controller for precise motions or tasks that may require contact of the robotic arm's end-effector with its environment. A low-performance (low-energy) controller could be used where less precise motion is needed. A command to set the processor clock was implemented in the joint controller. The low-performance mode with reduced processor clock led to a 3.5% energy savings compared to the high-performance clock rate.
In summary, assuming a nominal duty cycle for DEXARM of 75% in standby, 22.5% in low-performance motion and 2.5% in high-performance motion, the estimated total power savings using the methods implemented would be nearly 15%. Finally, an additional analysis and some tests have been conducted to evaluate the amount of power that can be saved when reducing PWM frequency. The result is a saving between 0.8 and 1.3 W when reducing PWM frequency from 20 kHz to 10 kHz.

JOINT TEST

The actual performance of the joint has been measured by means of the test equipment (MGSE/EGSE) described in [3]. The joint is mounted on a support structure (MGSE), while the output shaft is connected with an external high precision encoder by means of a very stiff shaft. This shaft can be connected to an external load.
Each joint has been subject to an extensive test campaign, including physical, electrical, functional and performance tests. The tests conducted have shown a very good behaviour. The functional performance has been verified in laboratory environment and under the specified operative thermal conditions, i.e. between –30°C and +70°C. The figures below report some brief examples of test results.

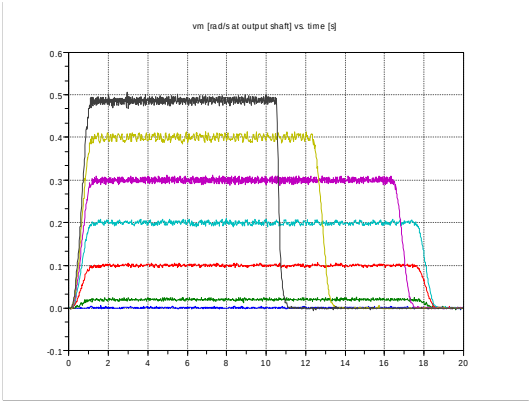

Fig. 9 Trajectory execution

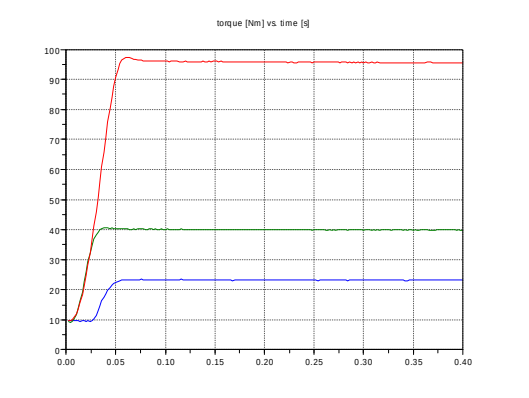

Fig. 10 Joint torque step response

Satisfactory performance has been obtained for each control loop. By an appropriate utilisation of the motor and output position sensors, the joint can perform smooth and accurate trajectories through a wide velocity range, from a very low velocity of $6.3 \cdot 10^{-6}$ rad/s (practically there is no lower limit) almost up to the theoretical limit of 0.5 rad/s. Positioning accuracy and repeatability are better than 0.025 degrees and 0.0025 degrees.

The choice of implementing the torque measurement in a "highly" stiff output flange led to a robust mechanical design. The sensitivity of the strain gauge measurement system resulted anyway good for guaranteeing torque control loop performance. The impact test (conducted for testing the torque loop) showed a stable impact and no bouncing. The manual backdrive test (either in torque control mode or in brake release mode) showed that it is possible to move the joint by hand.

ARM INTEGRATION AND TEST

The arm integration consists of the following main steps: inserting each joint electronics in a dedicated support cup, inserting the cable bundle in each joint (including joint and arm level cables), routing and fixing the cable bundle on both sides of the joint by means of the cable clamps, integrating together for each degree of freedom the joint, the electronics and the corresponding limb (or arm base).
Particular attention has been taken at arm design level towards maximum modularity and simplicity of integration. Some of the integration phases are shown in Fig. 11.

Fig. 11 Arm integration pictures

In order to perform coordinated joint and Cartesian motion, the arm will be connected to an external controller, composed of a computer board and a CAN bus interface board. The computer board will be equipped with the ESA CESAR/CONTEXT controller software, adapted for the DEXARM application (kinematics, CAN bus communication, etc).
The arm engineering model will be subject to a system test campaign, which includes physical, electrical, functional and performance tests. In particular, arm performance ISO-9283 parameters (as positioning accuracy, repeatability, etc.) will be evaluated using an optical measurement system. Finally, a vibration test (resonance survey) will be conducted in the proposed launch configuration (see Fig. 12).

Fig. 12 Vibration test set-up (CAD model)

CONCLUSION

An engineering model of DEXARM has been developed in phase 3 of the project.
The arm has been based on the most dexterous kinematics and geometrical configuration identified as output of the design phase. High performance and minimisation of resources have been pursued in any phase of the project for any components of the arm. Extensive design iterations were conducted for the joints, the electronics and the limbs, to minimise mass, dimensions and power, while ensuring the required performance. Particular attention has been given, already from the beginning, to make the design complete and to incorporate all features needed by higher level integrators to make use of the arm in the frame of their robotic systems.

The result is a dextrous robot arm that can be qualified and utilised in the frame of future ESA flight programmes.
After the execution of the system level tests, the arm will be delivered to ESA. System test results will be documented and made available. Next activities will be the integration with a tool exchange device (CTED, developed in the frame of ESA contract) and a robotic hand.

REFERENCES

[1] A. Rusconi, P. Magnani, T. Grasso, G. Rossi, J.F. Gonzalez Lodoso, G. Magnani, "*DEXARM – a Dextrous Robot Arm for Space Applications*", Proceedings of 8th ESA Workshop on Advanced Space Technologies for Robotics and Automation - ASTRA 2004, ESA/ESTEC, Noordwijk (The Netherlands), November 2004.

[2] P.H.M. Schoonejans, R. Stott, R, F. Didot, A. Allegra, E. Pensavalle, C. Heemskerk, "*Eurobot: EVA-assistant robot for ISS, Moon and Mars*", Proceedings of 8th ESA Workshop on Advanced Space Technologies for Robotics and Automation - ASTRA 2004, ESA/ESTEC, Noordwijk (The Netherlands), November 2004.

[3] A. Rusconi, P. Magnani, J. F. Gonzalez Lodoso, P. Campo, R. Chomicz, G. Magnani, *"Design and Development of an Integrated Joint for the Dextrous Robot Arm"*, Proceedings of 9th ESA Workshop on Advanced Space Technologies for Robotics and Automation - ASTRA 2006, ESA/ESTEC, Noordwijk (The Netherlands), November 2006.